



## Composite excitonic states in doped semiconductors

Dinh Van Tuan <sup>1</sup> and Hanan Dery <sup>1,2,\*</sup>

<sup>1</sup>Department of Electrical and Computer Engineering, University of Rochester, Rochester, New York 14627, USA

<sup>2</sup>Department of Physics and Astronomy, University of Rochester, Rochester, New York 14627, USA



(Received 21 February 2022; accepted 13 July 2022; published 9 August 2022)

We present a theoretical model of composite excitonic states in doped semiconductors. Many-body interactions between a photoexcited electron-hole pair and the electron gas are integrated into a computationally tractable few-body problem, solved by the variational method. We focus on electron-doped monolayer (ML)-MoSe<sub>2</sub> and ML-WSe<sub>2</sub> due to the contrasting character of their conduction bands. In both cases, the core of the composite is a tightly bound trion (two electrons and a valence-band hole) surrounded by a region depleted of electrons. The composite in ML-WSe<sub>2</sub> further includes a satellite electron with different quantum numbers. The theory is general and can be applied to semiconductors with various energy-band properties, allowing one to calculate their excitonic states and to quantify the interaction with the Fermi sea.

DOI: [10.1103/PhysRevB.106.L081301](https://doi.org/10.1103/PhysRevB.106.L081301)

Optical transitions in low-temperature doped semiconductors allow us to study many-body phenomena through the interaction between photoexcited electron-hole pairs and the Fermi sea [1–6]. For half a century, various theoretical models have been proposed to understand various observations. Mahan predicted singularity in optical conductivity due to interaction of Fermi-surface electrons with an infinite-mass valence-band (VB) hole [7,8]. This problem had direct connection with its contemporary x-ray edge problem due to excitation of deep core electrons in metals [9–12]. Two decades later, the problem was extended to one- and two-dimensional (2D) electron gases in semiconductor systems [13–18], along with the idea of shakeup processes [19–22].

Common to these early studies was the assumption of a relatively large Fermi energy, relevant in semiconductors when  $E_F \gg \varepsilon_T$ , where  $\varepsilon_T$  is gained energy from binding an exciton with a free electron to form a trion. The development of semiconductor nanostructures allowed researchers to study the physics of trions in the regime  $E_F \lesssim \varepsilon_T$  [23–25]. It was then suggested that the bare trion, a three-body complex, becomes correlated to the electron gas with the buildup of the Fermi sea [26–29]. The result is a four-body composite, termed a Suris tetron, in which the trion is bound to a Fermi hole in the conduction band (CB hole) [27]. Namely, the trion and the lack of Fermi-sea electrons in its vicinity move together. Following the discovery of monolayer transition-metal dichalcogenides (ML-TMDs) in the previous decade [30–36], the interest in this topic has been revived [37–44]. Borrowing from atomic systems [45,46], an alternative perspective to the observed behavior in ML semiconductors has been suggested. Rather than trions, excitons are viewed as mobile impurities in the electron gas, and the consequences of their interaction with the Fermi sea are repulsive and attractive Fermi polarons [47–50]. The latter is the equivalent of a trion.

In this letter, we describe a computational scheme through which many-body correlated excitonic states are converted to tractable few-body problems, solved by the variational method. The results shed light on optical measurements in ML semiconductors, providing support for the existence of excitonic states with a trion at their core surrounded by CB holes and satellite electrons if the electronic band structure supports it. Given the discrepancy with the Fermi-polaron picture, we find it important to emphasize from the outset why it is a trion rather than exciton at the core of these states. While the exciton binding energy is an order of magnitude larger than that of the trion,  $\varepsilon_X \gg \varepsilon_T$ , their spatial extents do not differ appreciably because the hole is equally and strongly bound to either of the two electrons [51–56]. The trion is glued by short-range forces between its three particles, where the total gained energy is  $\varepsilon_X + \varepsilon_T$ . The long-range dipolar force between an exciton and electron plays a secondary role. As such, and albeit  $\varepsilon_X \gg \varepsilon_T$ , it is misleading to think of a trion as a tightly bound exciton that is loosely held together with a satellite electron. The three particles of the trion remain strongly bound if the average distance between electrons in the Fermi sea exceeds the radius of the trion.

To make the discussion intelligible, we will focus on optical transitions in ML-MoSe<sub>2</sub> and ML-WSe<sub>2</sub> on account of their archetypal CB structures [57,58]. Figure 1(a) shows the photoexcitation process in electron-doped ML-MoSe<sub>2</sub>, where the core trion is accompanied by a CB hole. The two opposite-spin electrons exhaust the wave vector space above the Fermi surface,  $k \geq k_F$ , allowing them to orbit and bind the VB hole. On the other hand, the CB hole exhausts the  $k$ -space below the Fermi surface,  $k < k_F$ , and its spatial extent is commensurate with  $1/k_F$ . Hereafter, the combined core trion and CB hole is referred to as a *correlated trion* (or *tetron*). Its photoexcitation is accompanied by formation of an exchange-hole around the photoexcited electron, caused by exchange interaction between the photoexcited electron and electrons in  $-K$  [bandgap renormalization (BGR)]. The electron from the time-reversed

\*hanan.dery@rochester.edu

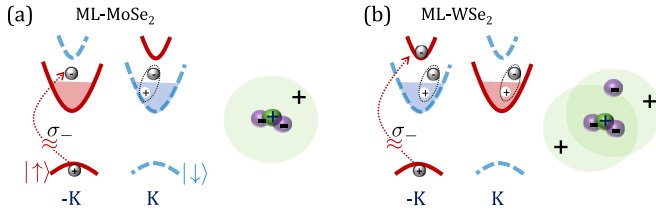


FIG. 1. Composite excitonic states in electron-doped monolayer (ML)-MoSe<sub>2</sub> and ML-WSe<sub>2</sub> following circularly polarized photoexcitation in the  $-K$  valley. The left diagrams in (a) and (b) show the corresponding  $k$ -space configurations. The right diagrams correspond to real-space configurations, showing a core trion surrounded by conduction band (CB) hole(s). The composite in ML-WSe<sub>2</sub> is further accompanied by a satellite electron. Each electron in these composites comes with distinct spin and valley quantum numbers.

valley at  $K$  is pulled out of the Fermi sea, resulting in a CB hole. This behavior is qualitatively like the one found in GaAs-based quantum wells in the sense that the spin and valley quantum numbers of the photoexcited electron are like those of electrons in the Fermi sea.

Electron-doped ML-WSe<sub>2</sub> is different. As shown in Fig. 1(b), the spin-valley quantum numbers of the photoexcited electron are distinct, allowing for the generation of a six-particle composite. The trion at its core comprises the VB hole and pulled-out electrons from the Fermi seas of the time-reversed valleys. The VB hole prefers binding tightly to these two electrons on account of their heavier mass compared with that of the optically active electron in the top valley [56,59]. The core trion is accompanied by two CB holes and the satellite photoexcited electron. The latter captures the electron-depleted region surrounding the core trion. When the electron density increases, the radius of the depleted region shrinks ( $\propto 1/k_F$ ), resulting in tighter binding of the top-valley electron to the rest of the complex. Hereafter, the six-particle composite is referred to as a *hexciton*.

Before embarking on the theory, we mention that this letter is part of a tetrad [60–62]. The first study that accompanies this letter is an analysis of magnetorelectance data in ML-WSe<sub>2</sub> [60]. We show that trions evolve to hexcitons and then to eight-body composites (oxcitons) when  $E_F$  crosses to the top valley of the CB. In addition, we analyze photoluminescence data and identify central and secondary optical transitions of hexcitons. The evidence we provide weakens our previous argument that exciton interaction with short-wave plasmons stands behind the observed optical transitions in electron-rich ML-WSe<sub>2</sub> [37,38,57,58]. The second study that accompanies this letter focuses on computational details of the theory [61], meant to help interested readers utilize the computational model and revisit similar physics in both nascent and good old semiconductors. The third study is a comprehensive analysis of correlated trions and hexcitons in ML-TMDs, where we further elaborate on the screened interaction with the electron gas [62]. This letter is the centerpiece of the theory, which we present next.

To account for the filling factor of Fermi-sea electrons, we use second quantization and write the Hamiltonian in momen-

tum space ( $\hbar = 1$ ):

$$H = K + V = \sum_{\mathbf{k}_\alpha} \frac{k^2}{2m_\alpha} c_{\mathbf{k}_\alpha}^\dagger c_{\mathbf{k}_\alpha} + \frac{1}{2} \sum_{\mathbf{k}_\alpha, \mathbf{p}_\beta, \mathbf{q}} V_{\alpha, \beta}(\mathbf{q}) c_{\mathbf{k}_\alpha + \mathbf{q}}^\dagger c_{\mathbf{p}_\beta - \mathbf{q}}^\dagger c_{\mathbf{p}_\beta} c_{\mathbf{k}_\alpha}, \quad (1)$$

where  $c_{\mathbf{k}_\alpha}^\dagger$  ( $c_{\mathbf{k}_\alpha}$ ) is the creation (annihilation) operator of an electron with momentum  $\mathbf{k}$ , and the index  $\alpha$  encompasses the band index, spin, and valley quantum numbers. Here,  $V_{\alpha, \beta}(\mathbf{q})$  is the Coulomb potential. Excitonic states are found from solutions of

$$HC = EOC. \quad (2)$$

Here,  $H_{ij} = \langle \phi_i | K + V | \phi_j \rangle$  and  $O_{ij} = \langle \phi_i | \phi_j \rangle$  are energy and overlap matrix elements, where  $\phi_i$  and  $\phi_j$  are basis states and  $C$  is a coefficient vector. Excluding the energy pocket of the photoexcited electron, CB electrons are assumed to be hosted in additional  $N$  energy pockets across the Brillouin zone, each with distinct spin-valley configuration. The resulting basis states of the composite read

$$|\phi_i\rangle = \sum_{\mathbf{X}} \phi_i(\mathbf{X}) c_{\mathbf{k}_0}^\dagger c_{v, \mathbf{p}_0} c_{\mathbf{k}_1}^\dagger c_{\mathbf{p}_1} \dots c_{\mathbf{k}_N}^\dagger c_{\mathbf{p}_N} |\phi_0\rangle, \quad (3)$$

where  $|\phi_0\rangle$  is the ground state of the system (filled electronic states up to the Fermi energy  $E_F$ ), the photoexcited VB hole comes from the first annihilation operator ( $c_{v, \mathbf{p}_0}$ ), and  $\mathbf{X} = \{\mathbf{k}_0, \mathbf{k}_1, \mathbf{p}_1, \mathbf{k}_2, \mathbf{p}_2, \dots, \mathbf{k}_N, \mathbf{p}_N\}$ , where the wave vector index embodies the unique valley-spin configuration of an electron in the complex. The pairs  $\mathbf{k}_i$  and  $\mathbf{p}_i$  denote a pulled-out electron and its CB hole. Here,  $\mathbf{k}_0$  is the wave vector of the photoexcited electron. In addition,  $\mathbf{p}_0 = \mathbf{k}_0 - \mathbf{Q} + \sum_\ell (\mathbf{k}_\ell - \mathbf{p}_\ell)$ , where  $\mathbf{Q}$  is the translation wave vector of the composite (constant of motion). The overlap matrix element is then

$$O_{ij} = \langle \phi_i | \phi_j \rangle = \sum_{\mathbf{X}} \phi_i^*(\mathbf{X}) \phi_j(\mathbf{X}) F(\mathbf{X}), \quad (4)$$

where  $\phi_{i(j)}(\mathbf{X})$  are basis functions, and the filling factor

$$F(\mathbf{X}) = f_{v, \mathbf{p}_0} (1 - f_{\mathbf{k}_0}) \prod_{\ell=1}^N (1 - f_{\mathbf{k}_\ell}) f_{\mathbf{p}_\ell} \quad (5)$$

is denoted in terms of Fermi distributions of electrons in the filled VB ( $f_{v, \mathbf{p}_0} = 1$ ) and CB energy pockets.

As is often the case, the computation becomes intractable already for small values of  $N$ . To circumvent this impasse, we first set the filling factor to  $F(\mathbf{X}) = 1$ , and later, we introduce the needed corrections to account for the  $k$ -space restrictions imposed by the Fermi distributions. The motivation for this approach is that the multivariable integration over  $\mathbf{X}$  can be carried analytically. We demonstrate the procedure by using Gaussian basis functions  $\phi_i(\mathbf{X}) = \exp(-\frac{1}{2} \mathbf{X}^T \mathbf{M}_i \mathbf{X})$ , where  $M_i$  is symmetric, real, and has a positive definite matrix of size  $(2N + 1) \times (2N + 1)$ . Setting  $F(\mathbf{X}) = 1$ , the overlap matrix elements become

$$O_{ij} = \left( \frac{A}{4\pi} \right)^{2N+1} \frac{1}{|M|}, \quad (6)$$

where  $A$  is the area of the 2D system,  $M = (M_i + M_j)/2$ , and  $|M|$  is its determinant. Focusing on the limit that  $Q = 0$ , in which the complex resides in the light cone, the kinetic-energy

matrix element due to relative motions of particles in the complex is

$$K_{ij} = \left( \frac{S_w}{2m_v} + \frac{w_0}{2m_e} + \sum_{\ell=1}^N \frac{w_\ell - w_{\bar{\ell}}}{2m_\ell} \right) O_{ij}, \quad (7)$$

where  $w_0 = W_{0,0}$ ,  $w_\ell = W_{\ell,\ell}$ , and  $w_{\bar{\ell}} = W_{\bar{\ell},\bar{\ell}}$  are diagonal elements of  $W = M^{-1}$ . The kinetic energy of the photoexcited electron is linked to  $w_0$ , and that of the VB hole to the sum of matrix elements in  $W$  ( $S_w$ ). Their respective masses are  $m_e$  and  $m_v$ . Similarly, the kinetic energy of the  $\ell$ th CB electron-hole pair is linked to  $w_\ell - w_{\bar{\ell}}$ , representing the electron energy above the Fermi level minus that of the missing electron below the Fermi level.

The potential-energy matrix elements between basis functions  $i$  and  $j$  are calculated from

$$V_{ij} = \sum_{\lambda=0, \lambda < \eta}^{2N} V_{ij}^{\lambda, \eta} + \sum_{\lambda=0}^{2N} V_{ij}^{\lambda}. \quad (8)$$

The first term is the interaction between two quasiparticles  $\{\lambda, \eta\}$ , and the second one is the interaction between quasiparticle  $\lambda$  and the VB hole. The former reads

$$V_{ij}^{\lambda, \eta} = \left[ \sum_{\mathbf{q}} V_{\lambda, \eta}(\mathbf{q}) \exp\left(-\frac{\gamma_{ij}^{\lambda, \eta} q^2}{2}\right) \right] O_{ij}, \quad (9)$$

where  $\gamma_{ij}^{\lambda, \eta} = D_{\lambda\lambda} + D_{\eta\eta} - D_{\lambda\eta} - D_{\eta\lambda}$ , with  $D = M_i - \frac{1}{2}M_i^T M^{-1} M_i$ , and  $M = (M_i + M_j)/2$ . The equation for  $V_{ij}^{\lambda}$  is the same but with  $\gamma_{ij}^{\lambda} = D_{\lambda\lambda}$ . The potential  $V_{\lambda, \eta}(\mathbf{q})$  is bare or screened, depending on the identity of the involved particles  $\lambda$  and  $\eta$ . The interaction between the three particles of the core trion are described by the bare (unscreened) Coulomb interaction because Fermi-sea electrons cannot screen their fast relative motion if  $a_T k_F \lesssim 1$ , where  $a_T$  is the trion radius. The resulting matrix element is

$$V_{ij}^{\lambda, \eta} = \frac{e_\lambda e_\eta}{2\epsilon_b r_0} e^{-x} [\pi \text{Erfi}(\sqrt{x}) - \text{Ei}(x)] O_{ij}, \quad (10)$$

where  $e_{\lambda(\eta)}$  is the charge of quasiparticle  $\lambda$  ( $\eta$ ),  $r_0$  is the polarizability of the 2D semiconductor,  $\epsilon_b$  is the dielectric constant of the barriers around the semiconductor, and  $x = \gamma_{ij}^{\lambda, \eta}/2r_0^2$ . Here,  $\text{Erfi}(x)$  and  $\text{Ei}(x)$  are imaginary error and exponential integral functions, respectively.

Other interactions, such as those between the core-trion particles and CB holes (or satellite electron), are weakly screened due to suppressed density fluctuations in the charge-depleted region around the core trion [62]. Elaborate analysis is provided in Ref. [61], including analytical expressions for matrix elements of the screened potential, of the exchange interaction between an electron and its CB hole, and of the BGR of the photoexcited electron.

Finally, the simplification made by setting  $F(\mathbf{X}) = 1$  is counteracted by introducing the potentials:

$$\begin{aligned} U_\ell(\mathbf{k}_\ell) &= \left( V_e - \frac{k_\ell^2}{2m_\ell} \right) \Theta(k_F - k_\ell), \\ U_{\bar{\ell}}(\mathbf{p}_\ell) &= \left( V_{\bar{e}} + \frac{p_\ell^2}{2m_\ell} \right) \Theta(p_\ell - k_F), \end{aligned} \quad (11)$$

for the  $\ell$ th electron and CB hole, respectively, where  $\Theta(q)$  is the Heaviside step function. In addition to fixing the kinetic energies, the energy constants  $V_e$  and  $V_{\bar{e}}$  are chosen large enough, so that the energy minimization process avoids solutions in which the  $\ell$ th electron penetrates the Fermi sea and its CB hole floats above the sea [63]. The correction matrix elements read

$$\begin{aligned} U_{ij} &= \left\{ \sum_{\ell=1}^N [1 - \exp(-\beta_\ell)] V_e + \exp(-\gamma_\ell) V_{\bar{e}} \right. \\ &\quad \left. + \frac{w_{\bar{\ell}} g_{\bar{\ell}}}{2m_\ell} - \frac{g_\ell w_\ell}{2m_\ell} \right\} O_{ij}, \end{aligned} \quad (12)$$

where  $\beta_\ell = k_{F, \ell}^2/w_\ell$ ,  $\gamma_\ell = k_{F, \ell}^2/w_{\bar{\ell}}$ ,  $g_\ell = 1 - \exp(-\beta_\ell)(1 + \beta_\ell)$ , and  $g_{\bar{\ell}} = \exp(-\gamma_\ell)(1 + \gamma_\ell)$ . Here,  $k_{F, \ell}$  is the Fermi wave number at the  $\ell$ th energy pocket.

The advantage of this computational method is that we work with small matrices instead of unwieldy multivariable integrals over the components of  $\mathbf{X}$ . One can then find the wave function of the composite:

$$\Psi(\mathbf{X}) = \sum_i C_i \exp\left(-\frac{1}{2} \mathbf{X}^T \mathbf{M}_i \mathbf{X}\right), \quad (13)$$

where the coefficients  $C_i$  and energy of the system are found by treating all elements of matrices  $M_i$  as variational parameters [61,64,65].

We use the model to quantify the ground-state binding energies of the correlated trion (tetron) and six-body hexciton as a function of electron density. The dielectric parameters and effective masses are modeled by assuming that ML-WSe<sub>2</sub> is encapsulated by hexagonal boron-nitride [62]. The conclusions we are about to make are qualitatively similar if we were to use effective masses and polarizability of ML-MoSe<sub>2</sub>. Figure 2(a) shows the energy of the correlated trion, calculated by using the bare (dashed line) and screened (solid line) potentials to describe the interaction between the CB hole and core trion [62]. The dotted line is the binding energy of the core trion, calculated with the restriction  $k > k_F$  for its electrons but without BGR and the CB hole. The energy decay of the core trion is evidently faster than the band-filling effect because it is harder for the VB hole to bind with faster electrons (large  $k$ ). The energy decay of the correlated trion at large densities is evidently weaker (solid and dashed lines), stemming from BGR of the photoexcited electron and offset between the reduced  $k$ -space of the other electron ( $k > k_F$ ) with increased  $k$ -space of its CB hole ( $k < k_F$ ). Experiments show that energy shifts of trion optical transitions are only moderately changed when charge is added to the semiconductor [43,44,66–68]. Comparing this behavior with our calculations, we see that a bare potential overestimates the binding energy of the CB hole at small charge densities, whereas the use of screened potential underestimates this binding at large charge densities. Further studies are needed to describe the correct screening effect of the electron gas [62]. We continue analyzing results calculated with the screened potential, bearing in mind that the discussion is qualitatively similar when using the bare potential. Figure 2(b) shows density distributions of particles in the correlated trion. The distributions of the electrons are

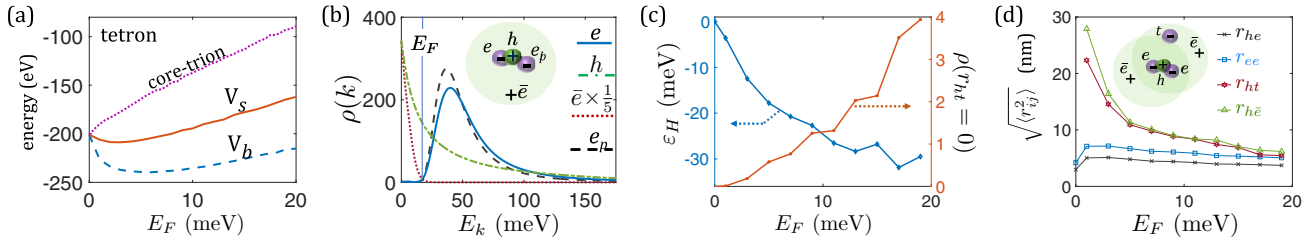


FIG. 2. (a) Tetron energy vs Fermi energy ( $E_F \approx 5$  meV amounts to electron density  $n = 10^{12}$  cm $^{-2}$ ). The dotted line is the contribution from the core trion [i.e., without bandgap renormalization (BGR) and the conduction band (CB) hole]. (b)  $k$ -space density distributions of particles in the tetron when  $E_F = 19$  meV. (c) Left: Binding energy of the satellite electron to the hexciton. Right: Overlap between valence band (VB) hole and satellite electron. (d) Interparticle distances in the hexciton, showing average distances within the core trion ( $r_{he}$  and  $r_{ee}$ ), between the VB hole and top-valley satellite electron ( $r_{ht}$ ), and between the VB and CB holes ( $r_{h\bar{e}}$ ).

not the same because the photoexcited electron is affected by BGR (dashed black line) and the other one by electron-hole exchange with its paired CB hole (solid blue line) [61]. The band-filling effect can be seen from their vanishing distributions below the Fermi energy. Conversely, the wave function of the CB hole vanishes above the Fermi energy (dotted red line). The VB hole has no  $k$ -space restriction (dashed-dotted green line).

Figure 2(c) shows the binding energy of the satellite electron in the hexciton composite (i.e., the ionization energy of the hexciton), calculated from the energy difference between six- and five-body composites. That the binding energy of the satellite electron grows with electron density is consistent with measurements of ML-WSe $_2$  [43,44,66,67], wherein the increase in electron density results in energy redshift and amplification of the dominant optical transition [60]. The redshift is analogous to increased binding energy, and the amplification to stronger overlap between the VB hole and photoexcited electron. As shown by Fig. 2(c), our calculations corroborate this behavior. Figure 2(d) shows average distances between particles in the hexciton. The core trion remains intact, as can be seen from the behavior of  $r_{he}$  and  $r_{ee}$ . The shrinkage of the CB holes when the charge density increases can be seen from the average distance between the VB and CB holes  $r_{h\bar{e}}$ . The behavior of  $r_{e\bar{e}}$  and  $r_{\bar{e}\bar{e}}$  is quantitatively similar [62]. The shrinkage of the CB hole further attracts the satellite electron to the core trion region, as can be seen from the behavior of  $r_{ht}$ .

Before concluding this letter, we mention two topics that merit further investigation. The first one deals with the strong blueshift experienced by the exciton optical transition when electrons (or holes) are added to the ML [43,44,66–68]. To

explain this behavior, we should introduce scattered states to couple correlated trions and excitons. Since energy levels of excitons reside in the continuum of trion states with finite kinetic energies, the result is a Fano-like resonance blueshift of the exciton optical transition. The second topic that merits further investigation deals with composite excitonic states in multivalley semiconductors such as Si or Ge. The relatively large dielectric constant in bulk semiconductors renders minuscule energy differences between the binding energies of composites with  $N$  and  $N + 1$  particles. Incorporating such materials in low-dimensional systems and encapsulating them in small-dielectric-constant environments are ways to enhance the binding energy and observe composites with relatively large  $N$ .

In conclusion, we have presented a theory of composite excitonic states in doped semiconductors. This important feat allows us to turn a rather difficult many-body problem into a computationally manageable few-body problem, which embodies the interaction between the electron gas and excitonic complexes. Using this method, we have calculated the tetron and hexciton states in ML-TMDs. Hopefully, the theory will help to sort out the ongoing debate on the origin of optical transitions in doped semiconductors and will spark a search for composite excitonic states in various multivalley semiconductors.

This letter was supported by the Department of Energy, Basic Energy Sciences, Division of Materials Sciences and Engineering under Award DE-SC0014349 (DVT) and by the Office of Naval Research under Award N000142112448 (HD).

- [1] H. Haug and S. Schmitt-Rink, Electron theory of the optical properties of laser excited semiconductors, *Prog. Quant. Electr.* **9**, 3 (1984).
- [2] S. Schmitt-Rink, D. S. Chemla, and D. A. B. Miller, Linear and nonlinear optical properties of semiconductor quantum wells, *Adv. Phys.* **38**, 89 (1989).
- [3] G. E. W. Bauer, Excitons in the quasi-two-dimensional electron gas, *Phys. Rev. B* **45**, 9153 (1992).
- [4] H. Haug and S. W. Koch, *Quantum Theory of the Optical and Electronic Properties of Semiconductors*, 3rd ed. (World Scientific, Singapore, 1994).

- [5] G. V. Astakhov, V. P. Kochereshko, D. R. Yakovlev, W. Ossau, J. Nurnberger, W. Faschinger, and G. Landwehr, Oscillator strength of trion states in ZnSe-based quantum wells, *Phys. Rev. B* **62**, 10345 (2000).
- [6] M. Combescot and S.-Y. Shiau, *Excitons and Cooper Pairs: Two Composite Bosons in Many-Body Physics* (Oxford University Press, Singapore, 2016).
- [7] G. D. Mahan, Excitons in degenerate semiconductors, *Phys. Rev.* **153**, 882 (1967).
- [8] G. D. Mahan, Excitons in metals: Infinite hole mass, *Phys. Rev.* **163**, 612 (1967).

- [9] P. W. Anderson, Infrared Catastrophe in Fermi Gases with Local Scattering Potentials, *Phys. Rev. Lett.* **18**, 1049 (1967).
- [10] P. Nozières and C. T. De Dominicis, Singularities in the x-ray absorption and emission of metals. III. One-body theory exact solution, *Phys. Rev.* **178**, 1097 (1969).
- [11] K. Schotte and U. Schotte, Threshold behavior of the x-ray spectra of light metals, *Phys. Rev.* **185**, 509 (1969).
- [12] M. Combescot and P. Nozières, Infrared catastrophe and excitons in the x-ray spectra of metals, *J. Phys. (Paris)* **32**, 913 (1971).
- [13] M. S. Skolnick, J. M. Rorison, K. J. Nash, D. J. Mowbray, P. R. Tapster, S. J. Bass, and A. D. Pitt, Observation of a Many-Body Edge Singularity in Quantum-Well Luminescence Spectra, *Phys. Rev. Lett.* **58**, 2130 (1987).
- [14] P. Hawrylak, Optical properties of a two-dimensional electron gas: Evolution of spectra from excitons to fermi-edge singularities, *Phys. Rev. B* **44**, 3821 (1991).
- [15] C. L. Kane, K. A. Matveev, and L. I. Glazman, Fermi-edge singularities and backscattering in a weakly interacting one-dimensional electron gas, *Phys. Rev. B* **49**, 2253 (1994).
- [16] S. A. Brown, J. F. Young, J. A. Brum, P. Hawrylak, and Z. Wasilewski, Evolution of the interband absorption threshold with the density of a two-dimensional electron gas, *Phys. Rev. B* **54**, R11082(R) (1996).
- [17] Alexander O. Gogolin, Alexander A. Nersesyan, and Alexei M. Tsvelik, *Bosonization and Strongly Correlated Systems* (Cambridge University Press, Cambridge, 2004).
- [18] V. V. Mkhitarian and M. E. Raikh, Fermi-Edge Singularity in the Vicinity of the Resonant Scattering Condition, *Phys. Rev. Lett.* **106**, 197003 (2011).
- [19] C. A. Swarts, J. D. Dow, and C. P. Flynn, Core Spectra of Metals, *Phys. Rev. Lett.* **43**, 158 (1979).
- [20] R. Sooryakumar, D. S. Chemla, A. Pinczuk, A. C. Gossard, W. Wiegmann, and L. J. Sham, Valence band mixing in GaAs-(AlGa)As heterostructures, *Solid State Commun.* **54**, 859 (1985).
- [21] Y.-C. Chang and G. D. Sanders, Band-mixing effect on the emission spectrum of modulation-doped semiconductor quantum wells, *Phys. Rev. B* **32**, 5521(R) (1985).
- [22] R. Sooryakumar, A. Pinczuk, A. C. Gossard, D. S. Chemla, and L. J. Sham, Tuning of the Valence-Band Structure of GaAs Quantum Wells by Uniaxial Stress, *Phys. Rev. Lett.* **58**, 1150 (1987).
- [23] K. Kheng, R. T. Cox, M. Y. d' Aubigné, F. Bassani, K. Saminadayar, and S. Tatarenko, Observation of Negatively Charged Excitons  $X^-$  in Semiconductor Quantum Wells, *Phys. Rev. Lett.* **71**, 1752 (1993).
- [24] G. Finkelstein, H. Shtrikman, and I. Bar-Joseph, Optical Spectroscopy of a Two-Dimensional Electron Gas Near the Metal-Insulator Transition, *Phys. Rev. Lett.* **74**, 976 (1995).
- [25] I. Bar-Joseph, Trions in GaAs quantum wells, *Semicond. Sci. Technol.* **20**, R29 (2005).
- [26] F. X. Bronold, Absorption spectrum of a weakly  $n$ -doped semiconductor quantum well, *Phys. Rev. B* **61**, 12620 (2000).
- [27] R. A. Suris, V. P. Kochereshko, G. V. Astakhov, D. R. Yakovlev, W. Ossau, J. Nurnberger, W. Faschinger, G. Landwehr, T. Wojtowicz, G. Karczewski *et al.*, Excitons and trions modified by interaction with a two-dimensional electron gas, *Phys. Stat. Sol. (b)* **227**, 343 (2001).
- [28] A. Esser, R. Zimmermann, and E. Runge, Theory of trion spectra in semiconductor nanostructures, *Phys. Stat. Sol. (b)* **227**, 317 (2001).
- [29] V. Koudinov, C. Kehl, A. V. Rodina, J. Geurts, D. Wolverson, and G. Karczewski, Suris Tetrons: Possible Spectroscopic Evidence for Four-Particle Optical Excitations of a Two-Dimensional Electron Gas, *Phys. Rev. Lett.* **112**, 147402 (2014).
- [30] A. Splendiani, L. Sun, Y. Zhang, T. Li, J. Kim, C.-Y. Chim, G. Galli, and F. Wang, Emerging photoluminescence in monolayer MoS<sub>2</sub>, *Nano Lett.* **10**, 1271 (2010).
- [31] K. F. Mak, C. Lee, J. Hone, J. Shan, and T. F. Heinz, Atomically Thin MoS<sub>2</sub>: A New Direct-Gap Semiconductor, *Phys. Rev. Lett.* **105**, 136805 (2010).
- [32] T. Korn, S. Heydrich, M. Hirmer, J. Schmutzler, and C. Schuller, Low-temperature photocarrier dynamics in monolayer MoS<sub>2</sub>, *Appl. Phys. Lett.* **99**, 102109 (2011).
- [33] H. Zeng, J. Dai, W. Yao, D. Xiao, and X. Cui, Valley polarization in MoS<sub>2</sub> monolayers by optical pumping, *Nat. Nanotechnol.* **7**, 490 (2012).
- [34] K. F. Mak, K. L. He, J. Shan, and T. F. Heinz, Control of valley polarization in monolayer MoS<sub>2</sub> by optical helicity, *Nat. Nanotechnol.* **7**, 494 (2012).
- [35] T. Cao, G. Wang, W. Han, H. Ye, C. Zhu, J. Shi, Q. Niu, P. Tan, E. Wang, B. Liu, and J. Feng, Valley-selective circular dichroism of monolayer molybdenum disulphide, *Nat. Commun.* **3**, 887 (2012).
- [36] A. M. Jones, H. Yu, N. J. Ghimire, S. Wu, G. Aivazian, J. S. Ross, B. Zhao, J. Yan, D. G. Mandrus, D. Xiao *et al.*, Optical generation of excitonic valley coherence in monolayer WSe<sub>2</sub>, *Nat. Nano.* **8**, 634 (2013).
- [37] H. Dery, Theory of intervalley Coulomb interactions in monolayer transition-metal dichalcogenides, *Phys. Rev. B* **94**, 075421 (2016).
- [38] D. Van Tuan, B. Scharf, I. Žutić, and H. Dery, Marrying Excitons and Plasmons in Monolayer Transition-Metal Dichalcogenides, *Phys. Rev. X* **7**, 041040 (2017).
- [39] M. Sidler, P. Back, O. Cotlet, A. Srivastava, T. Fink, M. Kroner, E. Demler, and A. Imamoglu, Fermi polaron-polaritons in charge-tunable atomically thin semiconductors, *Nat. Phys.* **13**, 255 (2017).
- [40] Y.-W. Chang and D. R. Reichman, Many-body theory of optical absorption in doped two-dimensional semiconductors, *Phys. Rev. B* **99**, 125421 (2019).
- [41] M. M. Glazov, Optical properties of charged excitons in two-dimensional semiconductors, *J. Chem. Phys.* **153**, 034703 (2020).
- [42] F. Rana, O. Koksals, and C. Manolatu, Many-body theory of the optical conductivity of excitons and trions in two-dimensional materials, *Phys. Rev. B* **102**, 085304 (2020).
- [43] E. Liu, J. van Baren, Z. Lu, T. Taniguchi, K. Watanabe, D. Smirnov, Y.-C. Chang, and C.-H. Lui, Exciton-polaron Rydberg states in monolayer MoSe<sub>2</sub> and WSe<sub>2</sub>, *Nat. Commun.* **12**, 6131 (2021).
- [44] J. Li, M. Goryca, J. Choi, X. Xu, and S. A. Crooker, Many-body exciton and intervalley correlations in heavily electron-doped WSe<sub>2</sub> monolayers, *Nano Lett.* **22**, 426 (2022).
- [45] B. Fröhlich, M. Feld, E. Vogt, M. Koschorreck, W. Zwerger, and M. Köhl, Radio-Frequency Spectroscopy of a Strongly

- Interacting Two-Dimensional Fermi Gas, *Phys. Rev. Lett.* **106**, 105301 (2011).
- [46] R. Schmidt, T. Enss, V. Pietilä, and E. Demler, Fermi polarons in two dimensions, *Phys. Rev. A* **85**, 021602(R) (2012).
- [47] D. K. Efimkin and A. H. MacDonald, Many-body theory of trion absorption features in two-dimensional semiconductors, *Phys. Rev. B* **95**, 035417 (2017).
- [48] D. K. Efimkin and A. H. MacDonald, Exciton-polarons in doped semiconductors in a strong magnetic field, *Phys. Rev. B* **97**, 235432 (2018).
- [49] C. Fey, P. Schmelcher, A. Imamoglu, and R. Schmidt, Theory of exciton-electron scattering in atomically thin semiconductors, *Phys. Rev. B* **101**, 195417 (2020).
- [50] Y.-C. Chang, S.-Y. Shiao, and M. Combescot, Crossover from trion-hole complex to exciton-polaron in  $n$ -doped two-dimensional semiconductor quantum wells, *Phys. Rev. B* **98**, 235203 (2018).
- [51] M. Z. Mayers, T. C. Berkelbach, M. S. Hybertsen, and D. R. Reichman, Binding energies and spatial structures of small carrier complexes in monolayer transition-metal dichalcogenides via diffusion Monte Carlo, *Phys. Rev. B* **92**, 161404(R) (2015).
- [52] I. Kylänpää and H.-P. Komsa, Binding energies of exciton complexes in transition metal dichalcogenide monolayers and effect of dielectric environment, *Phys. Rev. B* **92**, 205418 (2015).
- [53] D. W. Kidd, D. K. Zhang, and K. Varga, Binding energies and structures of two-dimensional excitonic complexes in transition metal dichalcogenides, *Phys. Rev. B* **93**, 125423 (2016).
- [54] M. Van der Donck, M. Zarenia, and F. M. Peeters, Excitons and trions in monolayer transition metal dichalcogenides: a comparative study between the multiband model and the quadratic single-band model, *Phys. Rev. B* **96**, 035131 (2017).
- [55] E. Mostaani, M. Szyniszewski, C. H. Price, R. Maezono, M. Danovich, R. J. Hunt, N. D. Drummond, and V. I. Fal'ko, Diffusion quantum Monte Carlo study of excitonic complexes in two-dimensional transition-metal dichalcogenides, *Phys. Rev. B* **96**, 075431 (2017).
- [56] D. Van Tuan, M. Yang, and H. Dery, Coulomb interaction in monolayer transition-metal dichalcogenides, *Phys. Rev. B* **98**, 125308 (2018).
- [57] B. Scharf, D. Van Tuan, I. Žutić, and H. Dery, Dynamical screening in monolayer transition-metal dichalcogenides and its manifestations in the exciton spectrum, *J. Phys.: Condens. Matter* **31**, 203001 (2019).
- [58] D. Van Tuan, B. Scharf, Z. Wang, J. Shan, K. F. Mak, I. Žutić, and H. Dery, Probing many-body interactions in monolayer transition-metal dichalcogenides, *Phys. Rev. B* **99**, 085301 (2019).
- [59] M. Yang, L. Ren, C. Robert, D. V. Tuan, L. Lombez, B. Urbaszek, X. Marie, and H. Dery, Relaxation and darkening of excitonic complexes in electrostatically-doped monolayer semiconductors: Roles of exciton-electron and trion-electron interactions, *Phys. Rev. B* **105**, 085302 (2022).
- [60] D. Van Tuan, S.-F. Shi, X. Xu, S. A. Crooker, and H. Dery, Six-Body and Eight-Body Exciton States in Monolayer WSe<sub>2</sub>, *Phys. Rev. Lett.* **129**, 076801 (2022).
- [61] D. Van Tuan and H. Dery, Turning many-body problems to few-body ones in photoexcited semiconductors using the stochastic variational method in momentum space, SVM- $k$ , [arXiv:2202.08378](https://arxiv.org/abs/2202.08378).
- [62] D. Van Tuan and H. Dery, Tetrons, pexcitons, and hexcitons in monolayer transition-metal dichalcogenides, [arXiv:2202.08379](https://arxiv.org/abs/2202.08379).
- [63] The chosen values of  $V_e$  and  $V_{\bar{e}}$  should be (i) much larger than the binding energy and (ii) such that the basis functions can describe the step function. A larger set of basis functions allows one to choose larger  $V_e$  and  $V_{\bar{e}}$ .
- [64] K. Varga and Y. Suzuki, Precise solution of few-body problems with the stochastic variational method on a correlated Gaussian basis, *Phys. Rev. C* **52**, 2885 (1995).
- [65] J. Mitroy, S. Bubin, W. Horiuchi, Y. Suzuki, L. Adamowicz, W. Cencek, K. Szalewicz, J. Komasa, D. Blume, and K. Varga, Theory and application of explicitly correlated Gaussians, *Rev. Mod. Phys.* **85**, 693 (2013).
- [66] Z. Wang, L. Zhao, K. F. Mak, and J. Shan, Probing the spin-polarized electronic band structure in monolayer transition metal dichalcogenides by optical spectroscopy, *Nano Lett.* **17**, 740 (2017).
- [67] T. Wang, Z. Li, Z. Lu, Y. Li, S. Miao, Z. Lian, Y. Meng, M. Blei, T. Taniguchi, K. Watanabe *et al.*, Observation of Quantized Exciton Energies in Monolayer WSe<sub>2</sub> Under a Strong Magnetic Field, *Phys. Rev. X* **10**, 021024 (2020).
- [68] T. Smoleński, O. Cotlet, A. Popert, P. Back, Y. Shimazaki, P. Knüppel, N. Dietler, T. Taniguchi, K. Watanabe, M. Kroner *et al.*, Interaction-Induced Shubnikov–de Haas Oscillations in Optical Conductivity of Monolayer MoSe<sub>2</sub>, *Phys. Rev. Lett.* **123**, 097403 (2019).